CHINESE OPTICS LETTERS

Vol. 22, No. 1 | January 2024

Simultaneous transmission of time-frequency and data with co-amplification over urban fiber links

Qian Cao (操 前)[1,2], Zhou Tong (童 周)[2], Lei Liu (刘 雷)[2], Jialiang Wang (王家亮)[2*], Kang Ying (应 康)[3], Fufei Pang (庞拂飞)[1], and Youzhen Gui (桂有珍)[2,4**]

[1] Key Laboratory of Specialty Fiber Optics and Optical Access Networks, School of Communication and Information Engineering, Shanghai University, Shanghai 200444, China

[2] Key Laboratory for Quantum Optics, Shanghai Institute of Optics and Fine Mechanics, Chinese Academy of Sciences, Shanghai 201800, China

[3] Key Laboratory of Space Laser Communication and Detection Technology, Shanghai Institute of Optics and Fine Mechanics, Chinese Academy of Sciences, Shanghai 201800, China

[4] Center of Materials Science and Optoelectronics Engineering, University of Chinese Academy of Sciences, Beijing 100049, China

*Corresponding author: jialiangking@siom.ac.cn

**Corresponding author: yzgui@siom.ac.cn

Received April 23, 2023 | Accepted August 31, 2023 | Posted Online December 29, 2023

We demonstrate a simultaneous transmission of time-frequency and data over a 160-km urban business network in Shanghai. The signals are transmitted through a cascaded optical link consisting of 48 km and 32 km, which are connected by an optical relay. The metrological signals are inserted into the communication network using dense wavelength division multiplexing. The influence of the interference between different signals has been discussed. The experimental results demonstrate that the radio frequency (RF) instability can reach 2.1×10^{-14} at 1 s and 2.3×10^{-17} at 10,000 s, and the time interval transfer of one pulse per second (1 PPS) signal with less than 10 ps at 1 s is obtained. This work paves the way for the widespread dissemination of ultra-stable time and frequency signals over the communication networks.

Keywords: simultaneous transmission; radio frequency transfer; communication network; wavelength multiplexing.
DOI: 10.3788/COL202422.011201

1. Introduction

High-precision time-frequency transfer has significant applications in atom clock comparison[1], navigation and positioning[2], 5th generation mobile networks[3], very long baseline interferometry[4], and other fields[5–7]. With the continuous development of modern atom clock technology, atom clocks have achieved unprecedented frequency stability, which is better than 1×10^{-13} at 1 s for the RF signal. The Global Navigation Satellite Systems (GNSS) enable time and frequency dissemination with near-global coverage. However, the stability of the RF signal is limited at a level around 1×10^{-15} over one day due to the environmental conditions[8,9]. Time and frequency transfer via optical fiber provides advantages such as high stability, low signal attenuation, and immunity to environmental factors that can affect RF signals. Furthermore, optical fiber networks have been widely deployed, providing a large and well-connected infrastructure that can be utilized for time and frequency transfer. These advantages make time-frequency transfer over optical fiber a promising solution for meeting the growing demand on high-precision time and frequency signaling.

Various methods for the transmission of time and frequency over the optical fiber links have been investigated[10–14]. By steering the frequency of an acousto-optic modulator (AOM), the stable transmission of frequency signals can be realized[15]. Although the stability of the RF signal is only 6.4×10^{-15} at 10,000 s, this scheme is compact in size with a robust performance. The phase fluctuations introduced by the link can be compensated by frequency mixing[16]. This passive phase correction method has a simple structure and good robustness. The scheme using dense wavelength division multiplexing (DWDM) has been proposed for time-frequency transmission, where the 9.1 GHz radio frequency stability is 7.0×10^{-15} at 1 s and 4.5×10^{-19} at 1 day at 80-km fiber link, and the precision of time synchronization is about 50 ps[17]. The system has been extended for simultaneous transmission of optical frequency reference, RF reference, and a 1 PPS (PPS, pulse per second) time signal[18]. However, these experiments are still conducted on dedicated fiber networks without data transmission.

Furthermore, parallel transmission of metrological signals with data communication by DWDM technology is also made. The scheme for simultaneously transferring metrological signals

with Internet data over a 540-km public telecommunication network has been constructed[19]. To reduce channel resource consumption, all optical signals are co-located in a single DWDM channel to reduce the optical bandwidth used for metrological signals[20]. The scheme for simultaneously transmitting stable time-frequency signals and data with a single wavelength has been proposed[21]. With active compensation based on an optical delay line, the frequency instability 5.9×10^{-17} at 10,000 s over a 106-km urban fiber link is obtained. Much excellent research has been done on long distance optical frequency[22], radio frequency[23,24], time[25,26], and simultaneous transmission[27–31]. All of the present research is focused on the joint transmission of metrological signals over longer or more complex optical fiber links. However, the analysis of interference between different signals is important for practical application. Compared to other simultaneous schemes, our proposed scheme offers a simple structure that is well-suited for long-distance transmission. Moreover, it exhibits strong scalability, making it convenient for network transmission and expansion.

In this paper, we demonstrate a simultaneous transmission of time-frequency and data with co-amplification over a 160-km urban business network in Shanghai. The metrological signals are inserted in the communication network using a DWDM scheme. The overlapping Allan deviation (OADEV) for the 2.2 GHz radio frequency achieves 2.1×10^{-14} at 1 s and scales down to 2.3×10^{-17} at 10,000 s, and the experimental results demonstrate that the proposed method can meet the requirements of transmitting ultra-stable time-frequency signals over a public communication network. We also analyze the effects of the interference between different signals with the common amplifiers. This work paves the way for the development of ultra-stable time-frequency network distribution in public telecommunication networks.

2. Implementation Principle and Experimental Setup

The DWDM schemes allow for the transmission of multiple optical signals on different predetermined slots of optical channels, which is commonly used in long-haul optical networks. The urban fiber link consists of three sites located at the Shanghai Institute of Optics and Fine Mechanics (SIOM), Chinese Academy of Sciences, the Shanghai Branch of Chinese Academy of Sciences (SHB), and the Shanghai Institute of Measurement and Testing Technology (SIMT). The location of these three sites is shown in Fig. 1.

The length of the urban fiber link between the SIOM and the SHB is 48 km, and the length between the SHB and the SIMT is 32 km. The total length of the urban fiber link is 160 km, with a loss of 52 dB, which is higher than the standard loss of laboratory fiber links due to unclean or aged connectors and fiber components. To avoid the degradation of transmission performance due to low received signal power, the bi-directional erbium-doped fiber amplifiers (Bi-EDFAs) are placed in the relay station (SHB).

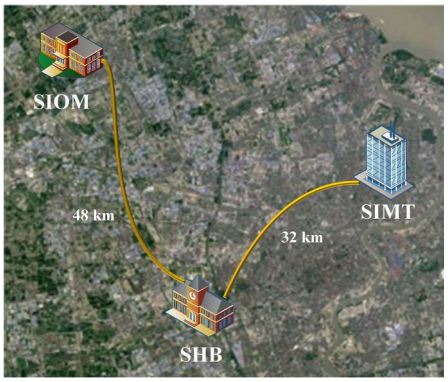

Fig. 1. Schematic of the urban fiber link connecting the SIOM, the SHB, and the SIMT.

To eliminate the effects of the environmental temperature changes and mechanical vibration on the stability of metrological signals in actual links, we propose the scheme for simultaneous transmission of time-frequency and Internet data, as shown in Fig. 2.

The simultaneous transmission scheme consists of three main components: the stable RF transmission, the accurate time transmission, and the data transmission. In the DWDM system, the wavelength spacing of the adjacent channels is 0.8 nm, and the power level of each channel is set to 6 dBm to avoid nonlinear effects. The specific composition of the transmission systems is depicted in Fig. 2. The local site (LS) and remote site (RS) are both located at the SIOM for ease of performance evaluation.

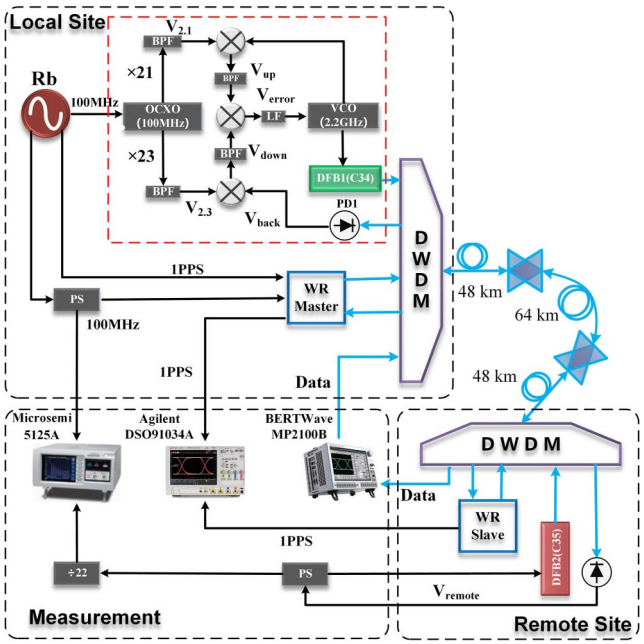

Fig. 2. General scheme of transmitting metrological signals with data in the public telecommunication network. BPF, bandpass filter; PD, photodetector; VCO, voltage-controlled oscillator; DFB, distributed feedback laser; LF, loop filter; PS, power splitter.

We will describe each transmission system component in the following paragraphs.

For RF transmission, an active compensation approach based on an electrical phase-lock loop (PLL) is adopted. The concrete composition of the solution is shown in the red box in Fig. 2. We use two distributed feedback (DFB) lasers with different wavelengths, 1550.1 nm (C34) and 1549.3 nm (C35), to suppress the impact of the mutual interference between the signals and the Rayleigh scattering during fiber transmission. The RF signals are modulated directly to the DFB lasers and the modulation depth is 0.51.

At the local site, the RF reference can be written as the following equation without regard to its exact amplitude for brevity:

$$V_{0.1} \propto \cos(\omega_{0.1} t + \varphi_{0.1}), \tag{1}$$

where $\omega_{0.1}$ is the angular frequency, and $\varphi_{0.1}$ is the initial phase.

After the signal is phase locked with a 100-MHz thermostatic crystal oscillator, the power is divided into two channels, with the frequency multiplied by 21 and 23, respectively. After passing a band-pass filter, two signals of 2.1 GHz and 2.3 GHz are obtained,

$$V_{2.1} \propto \cos(\omega_{2.1} t + \varphi_{2.1}), \tag{2}$$

$$V_{2.3} \propto \cos(\omega_{2.3} t + \varphi_{2.3}), \tag{3}$$

where $\omega_{2.1}$ and $\omega_{2.3}$ are the angular frequency, and $\varphi_{2.1}$ and $\varphi_{2.3}$ are the initial phase.

The frequency of the voltage-controlled oscillator (VCO) in the electrical compensation module is 2.2 GHz. The signal of VCO can be expressed as

$$V_{2.2} \propto \cos(\omega_{2.2} t + \varphi_{2.2}) \tag{4}$$

and is split into two parts. In that case, $\omega_{2.3} + \omega_{2.1} = 2\omega_{2.2}$, and $\varphi_{2.1} + \varphi_{2.3} = 2\varphi_{2.2}$. One branch of the $V_{2.2}$ signal is mixed with the $V_{2.1}$ signal to obtain

$$\begin{aligned} V_3 \propto & \cos[(\omega_{2.2} - \omega_{2.1})t + \varphi_{2.2} - \varphi_{2.1}] \\ & + \cos[(\omega_{2.2} + \omega_{2.1})t + \varphi_{2.2} + \varphi_{2.1}]. \end{aligned} \tag{5}$$

Then, V_3 is filtered by low-pass filters (LPFs) to obtain

$$V_{\text{up}} \propto \cos[(\omega_{2.2} - \omega_{2.1})t + \varphi_{2.2} - \varphi_{2.1}]. \tag{6}$$

The other branch of $V_{2.2}$ signal is modulated to the DFB laser and transmitted to the remote site, which is then detected by a photodetector (PD). Since the round-trip signal is transmitted over the same urban fiber link, the phase changes caused by the transmission over the fiber link can be assumed to be the same, and the signal transmitted back can be expressed as

$$V_{\text{back}} \propto \cos(\omega_{2.2} t + \varphi_{2.2} + 2\varphi_L). \tag{7}$$

Then, we mix the signal V_{back} with $V_{2.3}$ to obtain

$$V_{\text{down}} \propto \cos[(\omega_{2.2} - \omega_{2.1})t + \varphi_{2.2} - \varphi_{2.1} + 2\varphi_L]. \tag{8}$$

Mix the signals V_{up} and V_{down} to obtain a DC error signal

$$\begin{aligned} V_{\text{error}} \propto & \cos[(\omega_{2.3} + \omega_{2.1} - 2\omega_{2.2})t + \varphi_{2.1} + \varphi_{2.3} - 2\varphi_{2.2} \\ & + 2\varphi_L], \end{aligned} \tag{9}$$

and then simplify the equation to obtain

$$V_{\text{error}} \propto \cos(2\varphi_L). \tag{10}$$

The signal V_{error} undergoes proportional-integral-derivative (PID) processing to control the VCO, resulting in the generation of a phase shift of $-\varphi_L$ to obtain

$$V_{\text{remote}} \propto \cos(\omega_{2.2} t + \varphi_{2.2}). \tag{11}$$

Finally, we obtain a stable RF signal, which is then divided by 22, to match the reference 100 MHz signal. Then, the signals are injected into a phase-noise analyzer to evaluate the system performance.

Figure 2 also shows the system structure of the time transfer model. The time synchronization model adopts homemade time synchronization nodes based on the White Rabbit (WR) Project[32]. The WR protocol used for communication is compatible with the IEEE 1588v2 protocol, making it compatible with commercial data communication. The time signal is extracted from the transmitted communication digital signal, which is modulated to the optical carriers with wavelengths of 1548.5 nm (C36) and 1547.7 nm (C37) via the DWDM small form-factor pluggable (SFP) transceivers. The SFP is an integrated transceiver consisting of a laser, photodiode, and amplifier. The communication digital signal is on-off keying (OOK) modulated to the optical carriers. We measured the time delay drift results using a high-performance oscilloscope (Agilent DSO-91034A).

We use BERTWave MP2100B for data transmission and measurement. The BERTWave MP2100B is a commercial solution used for data transmission in an optical communications situation. It allows for high-speed data transfer with a tunable speed rate. In order to measure the bit-error-rate (BER), the BERTWave MP2100B is used to generate and detect 1.25 gigabits per second (Gbps) random code. For data transmission, the digital signal is also OOK modulated on the optical carriers with wavelengths of 1546. 9 nm (C38) and 1550.9 nm (C33) via the DWDM SFP transceivers. The digital signal is modulated on the optical carriers at the LS and demodulated at the RS via the SFP transceivers.

3. Results and Discussion

We measured the radio frequency transfer instability using a phase-noise analyzer (Microsemi TSC 5125A). Based on the

collected radio frequency data, the OADEV of the stable radio frequency transfer in a simultaneous transmission system is shown in Fig. 3. The red line shows the open loop performance of a 2.2 GHz radio frequency signal, which exhibits the instability of the RF as it reaches 1.3×10^{-13} at 1 s and then deteriorates to 1.1×10^{-13} at 10,000 s due to environmental temperature changes and mechanical vibrations. The blue line shows the closed-loop performance when the active noise compensation system is on. The instability of OADEV is 2.1×10^{-14} at 1 s and 2.3×10^{-17} at 10,000 s, which indicates that the proposed system can suppress the effects of environmental temperature changes and mechanical vibrations on the stability of the RF signal. To measure the noise floor of the system, we replaced the 160-km urban fiber link with a short fiber. The black line shows that the OADEV of the noise floor reaches 1.4×10^{-14} at 1 s and 1.5×10^{-17} at 10,000 s. It is demonstrated that the active noise compensation system works in a steady state.

The stability of the RF transmission outperformed the hydrogen maser. Therefore, the proposed system can achieve ultra-stable RF transmission over actual fiber links, enabling the development of atomic clock comparison and data communication.

We measured the time delay drifts using a high-performance oscilloscope (Agilent DSO91034A) regarding the 1 PPS time deviation (TDEV). 1 PPS means that a pulse signal is sent every second, and its role is to indicate the moment of the whole second.

Figure 4 shows the performance of the time transmission. The time deviation when the WR time is transferred alone over a 160-km fiber link reaches 6.8×10^{-12} at 1 s and 4.8×10^{-13} at 1000 s (blue line). The red line shows that the WR time is transferred along with the RF. It proves that the simultaneous transfer, along with the RF, does little interference to the WR signal. To measure the noise floor of the time transfer, we replaced the 160-km urban fiber link with a short fiber, and the result indicates that the TDEV reaches 5.3×10^{-12} at 1 s and 2.6×10^{-13} at 1000 s (black line). The bulge of the curves after 1000 s is due to the variation of the temperature. These results demonstrate that the proposed scheme can achieve highly stable time transfer over a long distance, making it suitable for applications such as atomic clock comparison and synchronization of communication systems.

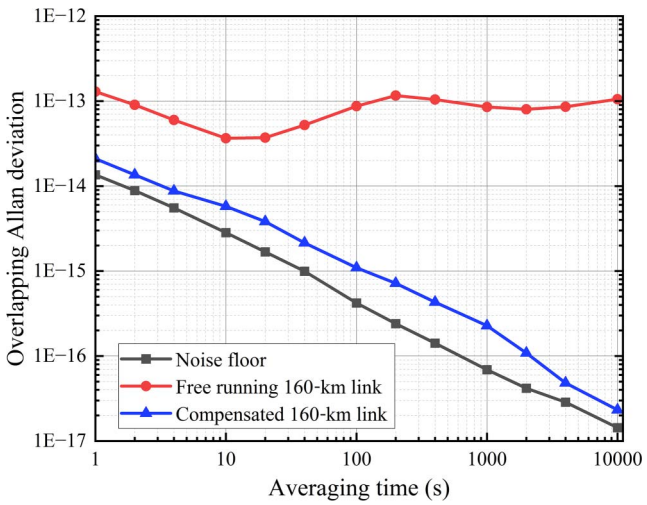

Fig. 3. Measured overlapping Allan deviation of the RF signal.

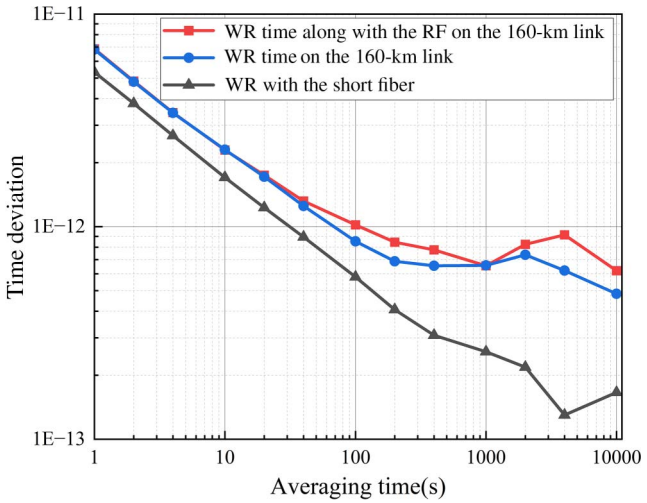

Fig. 4. Time deviation (TDEV) of the 1 PPS signal.

In order to analyze the mutual interference between the signals, the RF signal and the data signal are co-transmitted in a short fiber using the same amplifier. We change the power ratio of the RF signal to digital signals by adjusting the optical power of digital signals while keeping the optical power of the RF signal constant and evaluating the transmission instability of the RF signal under different power ratios. In order to depict the interference between signals, we chose the adjacent channels (C35, C36) to transmit metrological signals and data. Since the optical power of the received signal needs to be greater than −18 dBm, we need to choose the appropriate power ratio to avoid the SFP transceivers not working properly. Figure 5 shows the RF

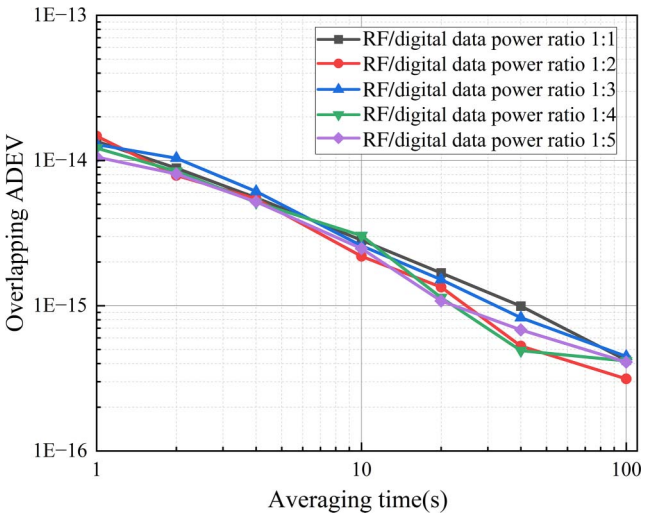

Fig. 5. Frequency instability (OADEV) of the RF signal with different input power ratios.

transfer performance in terms of different power ratios. We can see there is no noteworthy change in the stability of the RF signal within 100 s with different power ratios. Furthermore, there is no direct correlation between the measured frequency stability and the different signal power ratios within 100 s.

To further investigate the mutual interference between signals, we conducted the simultaneous transmission over a 160-km urban fiber link. Two sets of experiments were designed and compared: one for simultaneous transmission of the RF signal with digital signals and the other for the RF signal transmission only. The obtained instabilities (OADEV) of the RF signals in the two sets of experiments are shown in Fig. 6.

The black line in Fig. 6 represents the radio frequency transfer performance on the 160-km fiber link, which is almost consistent with that in the simultaneous transmission case (blue line) within 1–10 s. However, the stability of the RF signal in the co-transmission case deteriorated after 100 s. This could be due to changes in environmental conditions, such as temperature fluctuations during the measurement period. Therefore, the interference between different signals has little effect on the short-term frequency stability.

As for the data communication, the BER of the data communication is measured using the MP2100B at a data rate of 1.25 Gbps. The results show that the data BER is less than 1×10^{-12} when the received power was above the minimum threshold required for the SFP transceivers. These results demonstrate that the proposed scheme will not degrade the BER of the communication data. For the transmission of time-frequency signals over longer or more complex fiber optic links, the transmission distance limitation of the SFP transceiver and the polarization mode dispersion might be the challenges that we have to face. The SFP transceivers used here only support the maximum communication rate of 1.25 Gbps. To further increase the capacity of data transmission, more complex modulation or multiplexing methods can be used, such as quadrature amplitude modulation (QAM) or orthogonal frequency division multiplexing (OFDM).

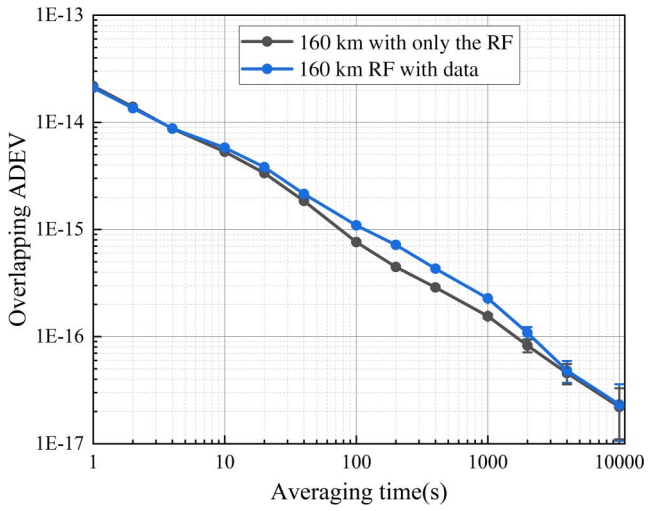

Fig. 6. Instability (OADEV) of the RF signal over a 160-km urban fiber link.

4. Conclusion

We demonstrate the simultaneous transmission of time-frequency and data over a 160-km urban business network in Shanghai. The results presented in this paper show that the proposed scheme can achieve high stability in both time and frequency domains. The stability of the radio frequency can reach 2.1×10^{-14} at 1 s and 2.3×10^{-17} at 10,000 s, which outperforms the stability of the hydrogen masers within the same time frame. The time deviation of 1 PPS is less than 10 ps at 1 s. When the received power is above the minimum threshold required for the SFP transceivers, the BER of data communication is less than 1×10^{-12}. The impact of the interference between different signals with the same amplifiers is also discussed. This work paves the way for the widespread dissemination of ultra-stable time and frequency signals over communication networks, enabling the development of precision measurement and the next generation of high-speed communication technology.

Acknowledgements

This work was supported by the National Key Research and Development Program of China (No. 2020YFB0408300), the National Natural Science Foundation of China (No. 62175246), the Natural Science Foundation of Shanghai (No. 22ZR1471100), and the Youth Innovation Promotion Association of the Chinese Academy of Sciences (No. YIPA2021244).

References

1. H. Marion, F. Pereira Dos Santos, M. Abgrall, *et al.*, "Search for variations of fundamental constants using atomic fountain clocks," Phys. Rev. Lett. **90**, 150801 (2003).
2. S. M. Foreman, K. W. Holman, D. D. Hudson, *et al.*, "Remote transfer of ultrastable frequency references via fiber networks," Rev. Sci. Instrum. **78**, 021101 (2007).
3. I. Krikidis, "Simultaneous information and energy transfer in large-scale networks with/without relaying," IEEE Trans. Commun. **62**, 900 (2014).
4. W. Schlüter and D. Behrend, "The International VLBI Service for Geodesy and Astrometry (IVS): current capabilities and future prospects," J. Geodesy **81**, 379 (2007).
5. B. J. Bloom, T. L. Nicholson, J. R. Williams, *et al.*, "An optical lattice clock with accuracy and stability at the 10^{-18} level," Nature **506**, 71 (2014).
6. T. Takano, M. Takamoto, I. Ushijima, *et al.*, "Geopotential measurements with synchronously linked optical lattice clocks," Nat. Photonics **10**, 662 (2016).
7. M. Tarenghi, "The Atacama Large Millimeter/Submillimeter Array: overview & status," Astrophys. Space. Sci. **313**, 1 (2008).
8. S. Weyers, V. Gerginov, M. Kazda, *et al.*, "Advances in the accuracy, stability, and reliability of the PTB primary fountain clocks," Metrologia **55**, 789 (2018).
9. W.-H. Tseng, S.-Y. Lin, K.-M. Feng, *et al.*, "Improving TWSTFT short-term stability by network time transfer," IEEE Trans. Ultrason. Ferroelectr. Freq. Control **57**, 161 (2010).
10. R. Wu, J. Lin, T. Jiang, *et al.*, "Stable radio frequency transfer over fiber based on microwave photonic phase shifter," Opt. Express **27**, 38109 (2019).
11. X. Zhu, B. Wang, Y. Guo, *et al.*, "Robust fiber-based frequency synchronization system immune to strong temperature fluctuation," Chin. Opt. Lett. **16**, 010605 (2018).

12. F. Yin, Z. Wu, Y. Dai, *et al.*, "Stable fiber-optic time transfer by active radio frequency phase locking," Opt. Lett. **39**, 3054 (2014).
13. H. Zhang, Y. Xiao, P. Qu, *et al.*, "Active delay stabilization of a 440-km fiber link in a wideband microwave delay system," IEEE Photon. J. **11**, 7100707 (2019).
14. G. Yang, H. Shi, Y. Yao, *et al.*, "Long-term frequency-stabilized optical frequency comb based on a turnkey Ti:sapphire mode-locked laser," Chin. Opt. Lett. **19**, 121405 (2021).
15. D. R. Gozzard, S. W. Schediwy, B. Courtney-Barrer, *et al.*, "Simple stabilized radio-frequency transfer with optical phase actuation," IEEE Photon. Tech. Lett. **30**, 258 (2018).
16. C. Hu, B. Luo, W. Pan, *et al.*, "Multipoint stable radio frequency long distance transmission over fiber based on tree topology, with user fairness and deployment flexibility," Opt. Express **28**, 23874 (2020).
17. B. Wang, C. Gao, W. L. Chen, *et al.*, "Precise and continuous time and frequency synchronisation at the 5×10^{-19} accuracy level," Sci. Rep. **2**, 556 (2012).
18. Q. Zang, H. Quan, K. Zhao, *et al.*, "High-precision time-frequency signal simultaneous transfer system via a WDM-based fiber link," Photonics **8**, 325 (2021).
19. O. Lopez, A. Haboucha, B. Chanteau, *et al.*, "Ultra-stable long distance optical frequency distribution using the Internet fiber network," Opt. Express **20**, 23518 (2012).
20. P. Krehlik, Ł. Śliwczyński, L. Buczek, *et al.*, "Optical multiplexing of metrological time and frequency signals in a single 100-GHz-grid optical channel," IEEE Trans. Ultrason. Ferroelectr. Freq. Control **68**, 2303 (2021).
21. Z. Lu, Y. Gui, J. Wang, *et al.*, "Fiber-optic time-frequency transfer in gigabit ethernet networks over urban fiber links," Opt. Express **29**, 11693 (2021).
22. K. Predehl, G. Grosche, S. M. F. Raupach, *et al.*, "A 920-kilometer optical fiber link for frequency metrology at the 19th decimal place," Science **336**, 441 (2012).
23. K. Turza, P. Krehlik, and Ł. Śliwczyński, "Compensation of the fluctuations of differential delay for frequency transfer in DWDM networks," IEEE Trans. Ultrason. Ferroelectr. Freq. Control **66**, 797 (2019).
24. N. Deng, Z. Liu, X. Wang, *et al.*, "Distribution of a phase-stabilized 100.02 GHz millimeter-wave signal over a 160 km optical fiber with 4.1×10^{-17} instability," Opt. Express **26**, 339 (2018).
25. B. Liu, X. Guo, W. Kong, *et al.*, "Stabilized time transfer via a 1000-km optical fiber link using high-precision delay compensation system," Photonics **9**, 522 (2022).
26. F. X. Chen, K. Zhao, B. Li, *et al.*, "High-precision dual-wavelength time transfer via 1085-km telecommunication fiber link," Acta Phys. Sin. **70**, 070702 (2021).
27. Q. Liu, S. Han, J. Wang, *et al.*, "Simultaneous frequency transfer and time synchronization over a 430 km fiber backbone network using a cascaded system," Chin. Opt. Lett. **14**, 070602 (2016).
28. F. Zuo, Q. Li, K. Xie, *et al.*, "Fiber-optic joint time and frequency transmission with enhanced time precision," Opt. Lett. **47**, 1005 (2022).
29. X. Guo, Y. Qiu, B. Liu, *et al.*, "A high-precision transfer of time and RF frequency via the fiber-optic link based on secure encryption," Appl. Sci. **12**, 6643 (2022).
30. L. Wang, Y. Liu, W. Jiao, *et al.*, "Fast and on-line link optimization for the long-distance two-way fiber-optic time and frequency transfer," Opt. Express **30**, 25522 (2022).
31. K. Turza, P. Krehlik, and Ł. Śliwczyński, "Long haul time and frequency distribution in different DWDM systems," IEEE Trans. Ultrason. Ferroelectr. Freq. Control **65**, 1287 (2018).
32. E. F. Dierikx, A. E. Wallin, T. Fordell, *et al.*, "White rabbit precision time protocol on long-distance fiber links," IEEE Trans. Ultrason. Ferroelectr. Freq. Control **63**, 945 (2016).